Clays and Clay Minerals, Vol. 67, No. 4:306−314, 2019

PREPARATION AND CHARACTERIZATION OF HIGH-VISCOSITY MONTMORILLONITE

Limei Wu[1], Xiaolong Wang[2], Changwei Xu[1] *, Fei Gao[1], Lili Gao[1], Guocheng Lv[3], and Li Yin[3]

[1]School of Materials Science and Engineering, Shenyang Jianzhu University, Shenyang 110168, China
[2]Procurement and Bidding Office, Shenyang Jianzhu University, Shenyang 110168, China
[3]School of Materials Science and Engineering, Jiangsu University of Science and Technology, Zhenjiang 212003, China

Abstract—Hydrophobicity, high viscosity, and dispersion are important properties for organo-montmorillonites, and all organo-montmorillonite configurations have yet to be fully characterized with respect to this property. High-viscosity montmorillonite (Mnt) is useful in gels and as an adsorber. The current study focused on modifying Mnt using organic cations and anions of various chain lengths in batch experiments with various concentrations and ratios. The viscosity of organic Mnt reached up to 395 mP.s. Molecular dynamics simulations and X-ray diffraction (XRD) were used to identify the conditions and arrangement of organic cations and anions in the Mnt interlayer area. The intercalation mechanism of organic cations and anions was also determined, providing a theoretical basis for the preparation of high-viscosity Mnt.

Keywords—Adsorption · Montmorillonite · Organic Intercalation · Viscosity

INTRODUCTION

Most clay minerals have peculiar adsorption arising from their layered structure, charged layers, and active edges (Zhou & Keeling 2013). Clay minerals include distinct nm-scaled layers and interlayers that can be engineered as selective and active adsorbents and catalysts (Zhou et al. 2016). Mnt is a natural mineral with a nanoscale 2:1 layer structure. In a tetrahedral Mnt crystal, a few Si^{4+} ions are replaced by Al^{3+}, and similarly in an octahedral crystal, a few Al^{3+} positions are replaced by Mg^{2+} (Yoshimoto et al. 2005; Zhou 2011). Both replacements render a permanent negative charge in the Mnt layer; thus cations such as Na^+ and Ca^{2+} must be adsorbed to maintain a balanced structural charge (Lagaly 1982; Wu et al. 2014a). Mnt has a large cation exchange capacity (CEC). These cations can be replaced by other inorganic or organic cations, which is an effective way to construct ordered inorganic-organic and inorganic-inorganic assemblies with unique microstructures and properties. Mnts have attractive features, such as large surface area, swelling behavior, adsorption, and ion-exchange properties (Zhou et al. 2019). Organic modification is based on cationic exchangeability in Mnt. For example, the capacity of Mnt to adsorb CTAB (hexadecyl trimethyl ammonium bromide or cetyltrimethylammonium bromide) can reach 1300 mmol/kg (Zhou et al., 2014). A Mnt particle consists of thousands of basic crystal units in a single layer, and the activity and mutability at the particle surface and the interlayer space and within a layer are different (Jeschke Meleshyn 2011).

A Mnt/alkyl ammonium composite is a novel mineral prepared by replacing interlayer exchangeable metallic cations in Mnt with alkyl quaternary ammonium organic cations (Pospíšil et al. 2003; Alemdar et al. 2005). Alkyl ammonium cation intercalation/adsorption changes natural Mnt from hydrophilic into a hydrophobic mineral, making it compatible with organic substances (Kwolek et al. 2003). This modification allows Mnt to be used in composite materials to form a thixotropic gel in an organic solvent, oil, or liquid resin; this gel can then adsorb organic contaminants in water (Vassilios et al. 2009; Zhou et al. 2011; Martín Alfonso et al. 2014). Therefore, composite materials prepared via organic modification have potential applications in various areas, including paints, coatings, cosmetics, fats, oil-based drilling mud, nanopolymers, and materials for controlling water pollution (Yalçin et al. 2002; Menezes et al. 2010). The amount of alkyl ammonium intercalation in Mnt is determined primarily by the type of Mnt (i.e. the charge on a Mnt cell), species of adsorbed ions, pH of the solution, and particle distribution of Mnt (Lv et al. 2012). Adsorption on a surfactant provides ion exchange, ion pairing, hydrogen bonding, electron polarization, dispersive forces, and hydrophobicity (Kaci & Chaouche 2011). Various approaches have been used to improve gel performance of organic-modified Mnt. In order to improve the composite material performance in paints and drilling mud, researchers attempted to increase the adsorption capacity with the goal of increased intercalation and increased viscosity (Yu et al. 2014)

Using alkylammonium alongside another reagent as a modifier for Mnt has a better effect in terms of modification than raw Mnt. Quaternary ammonium and an organic or inorganic agent are most commonly used in this process. Combining a cationic and other ionic agent to increase the viscosity of organic Mnt has been shown to be an effective method. The purpose of the present study was to use organic cations and anions to prepare modified Mnt with high viscosity, and to determine the optimal combination ratio, concentration, solution pH, and organic chain length.

---

* E-mail address of corresponding author: 1301663317@qq.com
DOI: 10.1007/s42860-019-00024-1

This paper was originally presented during the World Forum on Industrial Minerals, held in Qing Yang, China, October 2018

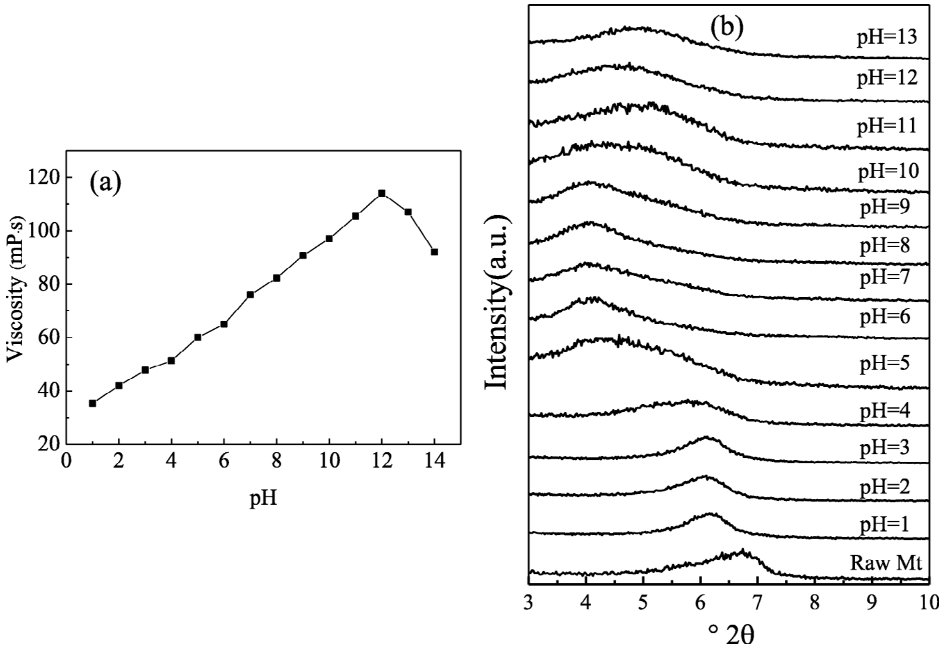

Fig. 1 (**a**) The viscosity of CTAB-Mnt at various pH values; and (**b**) XRD patterns of CTAB-Mnt at various pH values

EXPERIMENTAL WORK

Materials

The Mnt used was obtained from the Source Clays Repository of The Clay Minerals Society. Details of the Mnt were given in a previous work (Wu et al. 2014b).

The hexadecyl trimethyl ammonium bromide (CTAB) (57-09-0), myristyl trimethyl ammonium bromide (TTAB) (1119-97-7), dodecyl trimethyl ammonium bromide (DTAB) (1119-94-4), octyl trimethyl ammonium bromide (OTAB) (2083-68-3), sodium dodecyl sulfate (SDS) (151-21-3) and sodium hexadecyl sulfate (SHS) (1120-01-0) were provided by Sinopharm Chemical Reagent Beijing Co., Ltd (Beijing, China).

Experiment

Mnt was placed in distilled water to prepare a slurry having a solids content of 6% Mnt. A mixed solution of CTAB and SDS was then prepared. The slurry prepared was stirred, and the mixed solution added to it. The sample was then placed in a water bath and stirred at 40°C for 3 h. After completion of the stirring, the mixture was centrifuged at 5000 rpm (3800×g) for 10 min to separate the liquid from the solid parts. The solid sample obtained was dried at 60°C for 5 h and then ground to a powder by hand using a mortar and pestle.

Characterization

Powder X-ray diffraction (XRD) analyses were performed using a Rigaku D/max-IIIa diffractometer (Tokyo, Japan) (Cu Kα operating at 80 mA and 60 kV at a scan rate of 2°2θ/min. The sample was placed on a sample table. The directional scanning process proceeded from 3 to 70°2θ with the angle gradient of each scan of ~0.02°2θ. The change in intensity of d_{001} of Mnt was measured in order to estimate the intercalation effect and the d value was calculated according to the Bragg equation.

The viscosity of organic-Mnt was measured using a HAAKE RotoViscol rheometer (Karlsruhe, Germany). The shear rates were 0 s^{-1} to ~200 s^{-1} and 200 s^{-1} to ~0 s^{-1} for 3 min at a constant temperature of 20°C. The data collected were matched automatically by computer, the relation curve between shear stress and shear rate was drawn, and then the area of the thixotropic loop between the upward curve and the downward curve was determined by integration.

The powder sample was dispersed in ether by ultrasonic wave for 30 min. The powder samples were then analyzed by transmission electron microscopy (JEM-2100FSTEM/EDS. JEOL) (Tokyo, Japan) using an accelerating voltage of 160–200 kV and magnification of 50,000–1,100,000.

Molecular simulation was performed under the module 'Forcite' of *Materials Studio* 7.1 software to investigate the sorption sites of CTAB and SDS on Mnt. The resulting primitive unit cell was characterized by the parameters a = 15.540 Å, b = 17.940 Å, c = 12.88 Å, and $\alpha = \gamma = 90°$, $\beta = 99°$. Based on the primitive unit cell, a series of (6×4×2) supercells was built with the spacing of layers set to 12.88 Å.

Based on the structure of the preferential adsorption model of CTAB and SDS in the layer of Mnt predicted by Monte Carlo (MC) calculation, GGA-PW91 was used to optimize the structure again and to predict more accurately the interaction energy between SA and Mnt layers. All of the GGA-PW91 calculations were performed using a double numerical plus polarization function (DNP) as basis set and DFT-D correction. For all calculations, the

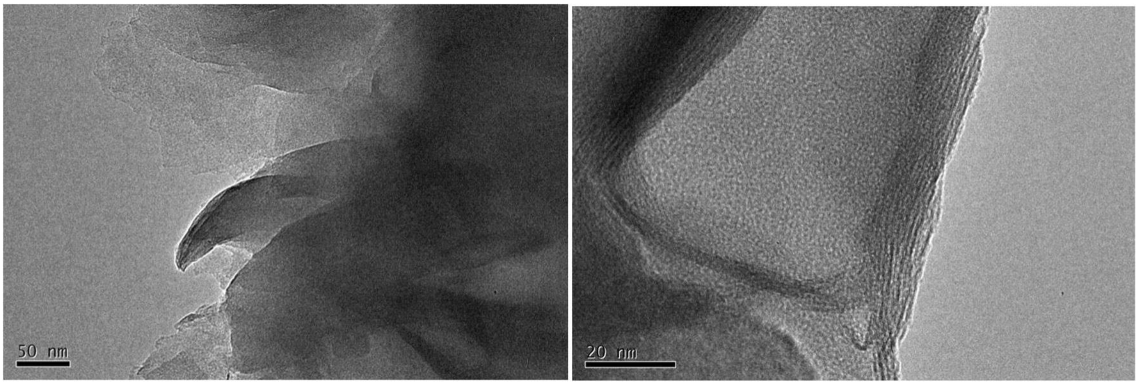

Fig. 2 TEM images of CTAB-Mnt

heavy atoms of Mnt were frozen, whereas the hydrogen of Mnt cationic molecules was fully relaxed.

RESULTS AND DISCUSSION

Preparation and Characterization of High-viscosity Organic Mnt

Influence of pH CTAB is a cationic organic surfactant with constant positive charge in solution at any pH. CTAB enters the Mnt interlayer space through cation exchange to produce CTAB-modified Mnt. Intercalation of CTAB into Mnt was minimized when Mnt was modified at pH 4 with a given CEC value of CTAB (Fig. 1). This is because CTAB is positively charged in an acidic solution, thus it acidifies the Mnt and dissolves some of the Si from the tetrahedral sheet and/or Al from the octahedral sheet, rendering greater layer charge and making cation exchange more difficult (Wungu et al. 2011; Wu et al. 2014c). This results in a small degree of intercalation of organic cations.

Introduction of CTA$^+$ cations into interlayer spaces in Mnt increases the basal spacing in the resultant solid (Yu et al. 2014;

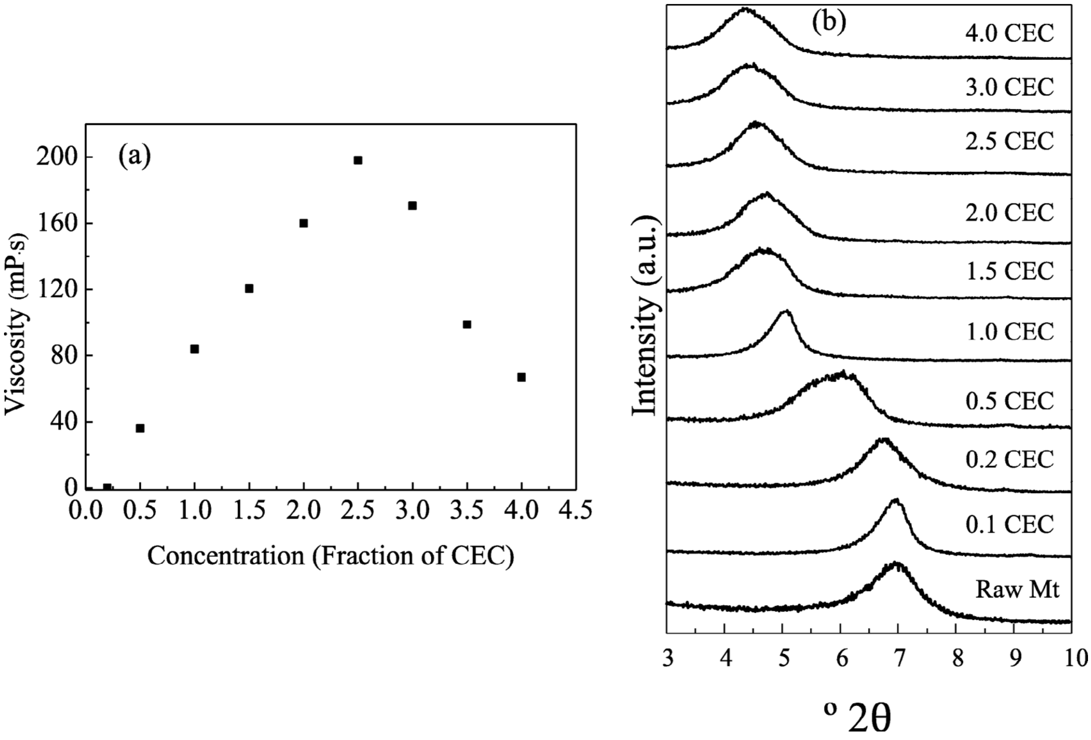

Fig. 3 (**a**) The viscosity of CTAB-Mnt at various C_{16}mimCl concentrations; and (**b**) XRD patterns of CTAB-Mnt at various CTAB concentrations

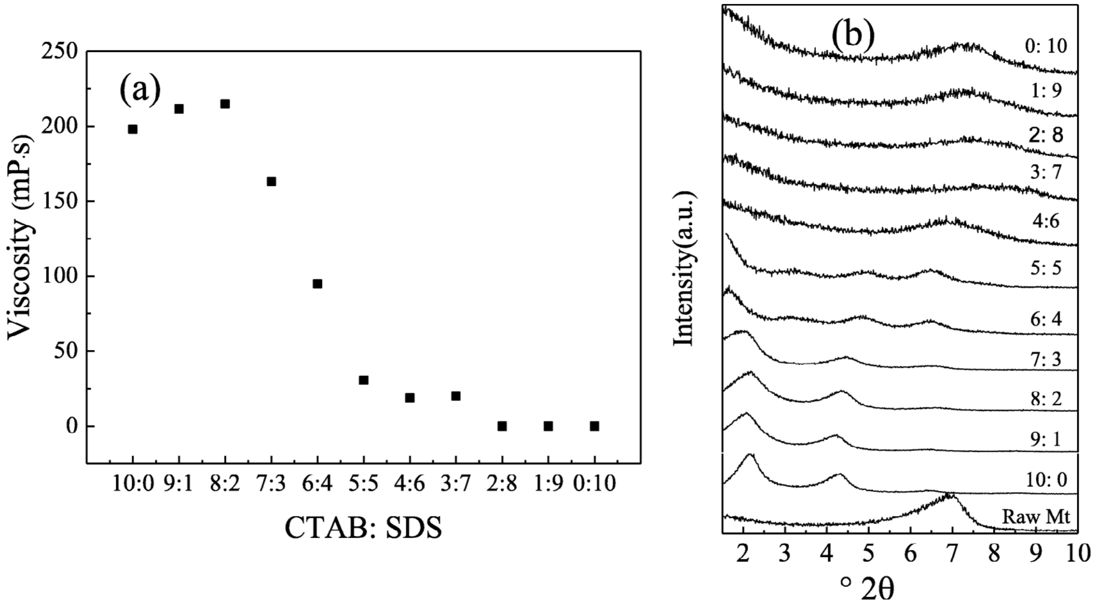

Fig. 4 (**a**) The viscosity of SDS-CTAB-Mnt at various ratios of CTAB and SDS; and (**b**) XRD patterns of SDS- CTAB-Mnt at various ratios of CTAB and SDS

Yu et al. 2017). In contrast, intercalation of CTAB in Mnt also increased when the pH increased from 5 to 9, and d_{001} was as large as 22.5 Å at pH 9. Intercalation decreased as the solution became more alkaline above pH 9 because CTAB is neutralized after combining with OH^- in solution. The force driving formation of a neutral molecule is quite weak, however, so it is possible for the remaining CTAB to enter the Mnt interlayer (Ouhadi et al. 2006; He et al. 2006). The permanent layer charge, hydrophobicity, and Van der Waals forces are present during organic intercalation (Yu et al. 2017). Others have verified that 60–80% of the driving force is due to cation exchange (i.e. layer charge), while 20–40% of the driving force is due to the hydrophobicity of organic cations during intercalation of organic cations with Mnt (Wu et al. 2014d).

Organic Mnt composites prepared in acidic solution have relatively low viscosity (<100 mP·s). In contrast, the viscosity

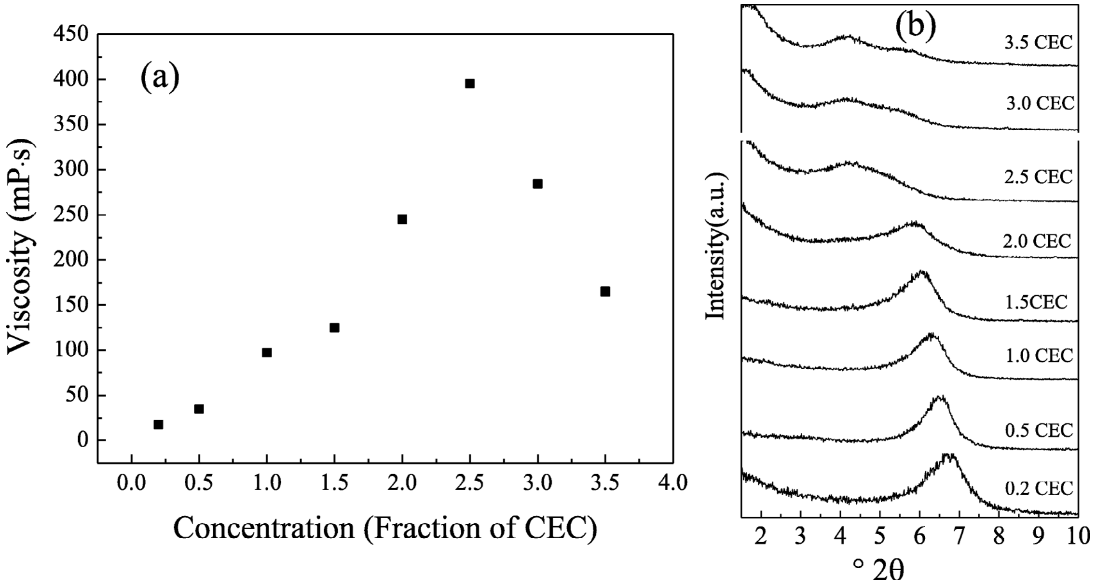

Fig. 5 (**a**) The viscosity of SDS-CTAB-Mnt at various SDS and CTAB concentrations; and (**b**) XRD patterns of SDS-CTAB-Mnt at various SDS and CTAB concentrations

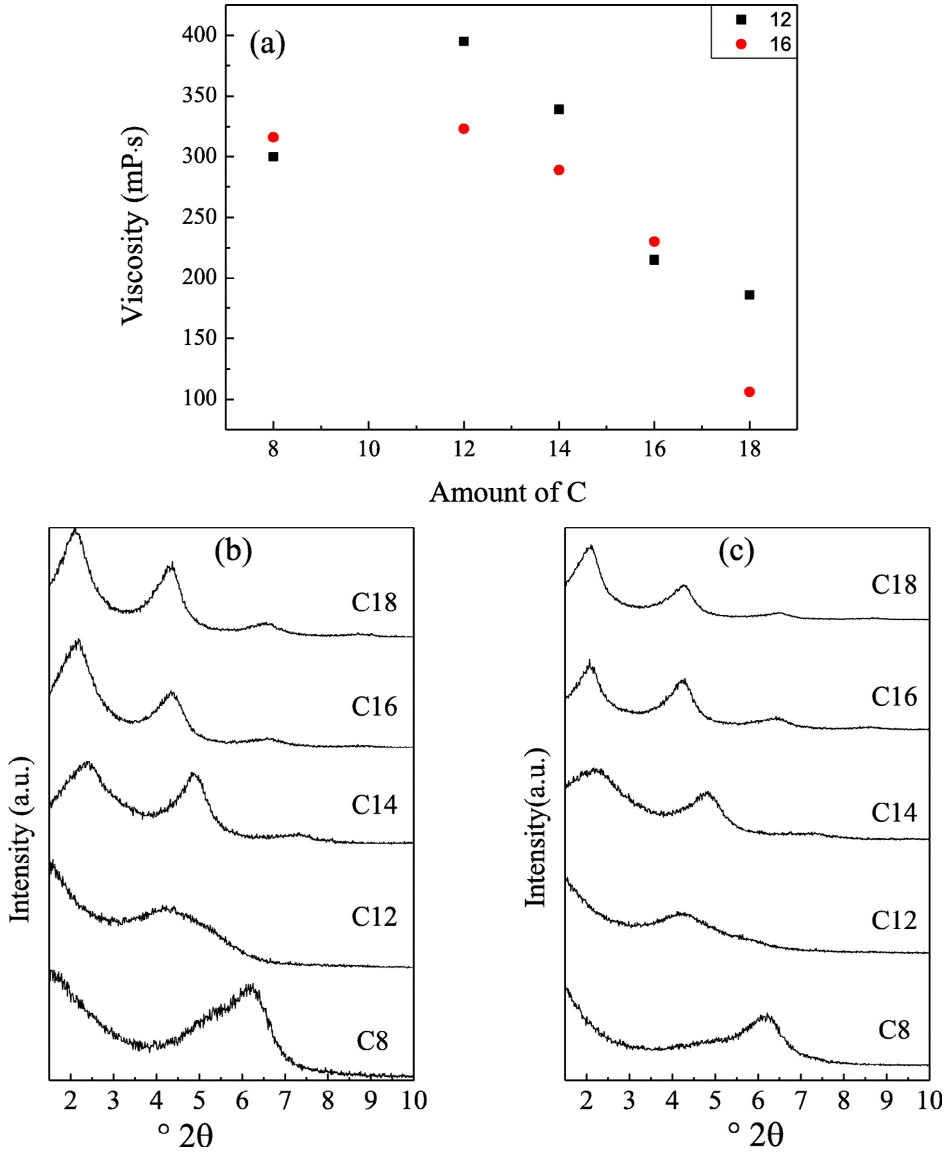

Fig. 6 The viscosity of SDS-CTAB-Mnt at various chain lengths of organics (**a**); XRD patterns of anion-cation-Mnt at various chain-length of cation organics, SHS (**b**); and SDS (**c**)

of organic Mnt increases as the basicity of the solution increases, reaching 114 mP·s at pH 12. This indicates that an alkaline solution is optimal for preparing organic Mnt with high viscosity. TEM images of CTAB-Mnt showed the multilayer structure in Mnt (Fig. 2). The interlayer spacing of the CTAB-Mnt was ~20 Å, which is consistent with the XRD results.

Influence of Organic Cation Concentration The concentration of organic cations is a key factor for controlling intercalation of organic cations in Mnt (Zhou et al. 2009). Increasing the concentration of cations (shown as multiples of CEC in Mnt) effectively increases intercalation of organic cations. The interlayer spacing in Mnt increased as the organic cation dosage increased, indicating increased intercalation (Fig. 3). Intercalation approached equilibrium at 1.5 CEC for organic cations. Subsequently, the interlayer spacing increased only slightly despite the considerable dosage of cations (Bumbudsanpharoke et al. 2017). However, the (001) diffraction peak becomes sharp, indicating that changes occur in the interlayer arrangement of cations; specifically, the arrangement tended to be more uniform and stable (Austin et al. 2018). Consequently, the dose of organic cations affects intercalation and the interlayer arrangement of intercalated organic cations in Mnt (Wu et al., 2014a; Karataş et al. 2017).

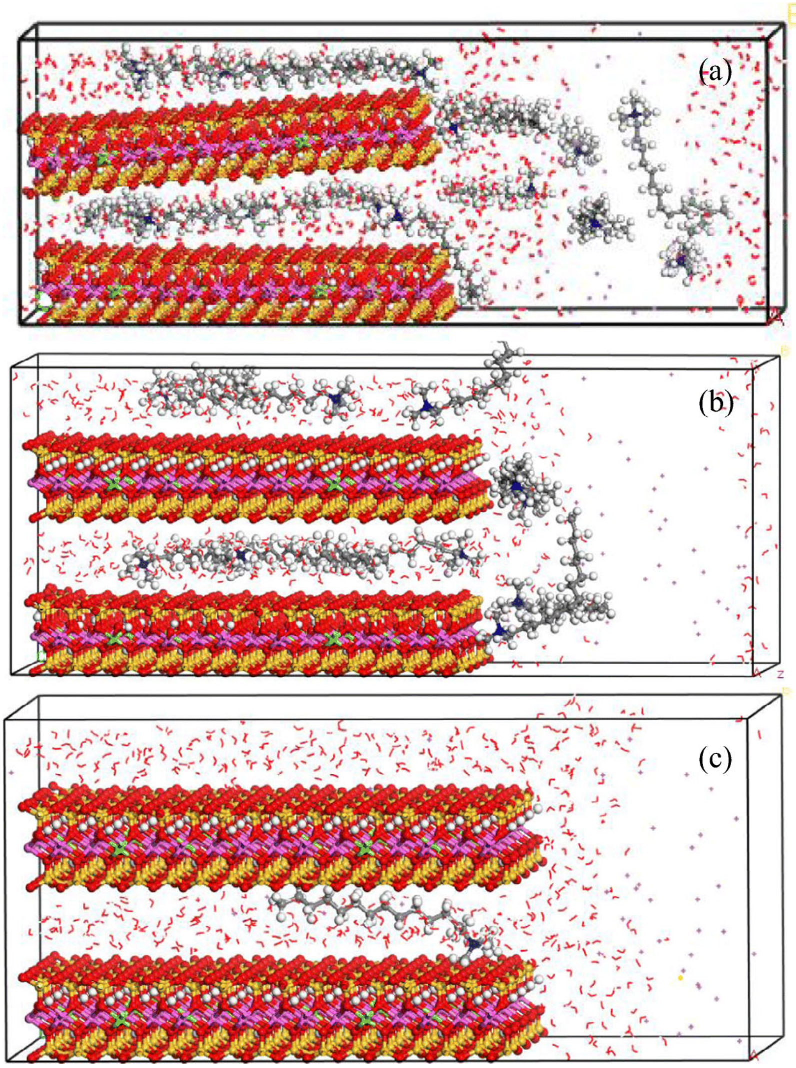

Fig. 7 Molecular dynamics simulations of CTAB-Mnt at various CTAB concentrations: (**a**) 4 CEC, (**b**) 2.5 CEC, and (**c**) 0.2 CEC

The viscosity of the organic-modified Mnt increased as the CTAB concentration increased, and the viscosity was highest with 2.5 CEC concentration of CTAB. Equilibrium intercalation appeared at a CTAB concentration of 1.5 CEC. The viscosity increased continuously as the CTAB dose increasesd and the highest viscosity was 198 mP·s. The experimental results suggest a correlation between the viscosity of Mnt and intercalation, as well as organicization of the outer surface.

Influence of the ratio of organic cations to anions Modifying Mnt with a single CTAB solution did not yield composites with high viscosity. To increase the viscosity, anionic organic SDS was used in this study with CTAB to modify Mnt (Fig. 4). The doses and ratio of CTAB to SDS have different effects on modification. Organic cations used for modification exchange with interlayer cations in Mnt, whereas organic anions are adsorbed only on the surface of Mnt and do not exchange with interlayer ions (Gűngőr et al. 2001; Günister et al. 2006).

The interlayer spacing (d_{001}) of Mnt increased to 32 Å as the ratio of CTAB to SDS decreased from 10:0 to 5:5. Interlayer hydrated cations such as $Na \cdot H_2O^+$ (Zhu et al. 2019) can be exchanged by CTAB and SDS, which increases d_{001} because CTAB and SDS are larger molecules than other hydrated cations. However, decreasing the ratio further led to a decrease in the interlayer spacing, and d_{001} decreased to 26 Å, suggesting that maximum intercalation could be achieved only with a certain ratio of CTAB to SDS. Organic anions may impede interactions between organic cations and Mnt, thus reducing its organicization (İşçi et al. 2005).

The ratio of CTAB to SDS has a significant impact on the viscosity of the modified Mnt solution. Organic Mnt has the

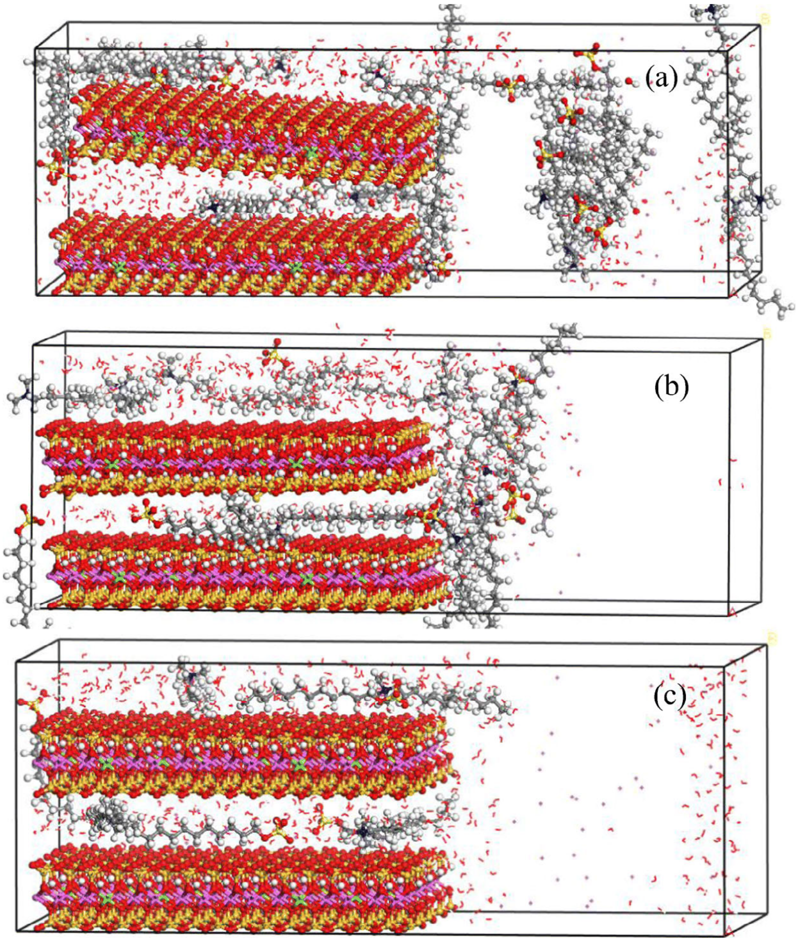

Fig. 8 Molecular dynamics simulations of SDS-CTAB-Mnt at various SDS and CTAB concentrations: (**a**) 4 CEC, (**b**) 2.5 CEC, and (**c**) 1.0 CEC

highest viscosity (211 mP·s) at a 9:1 ratio of organic cation to anion, and the viscosity decreased as the ratio decreased.

Influence of organic anion concentration The concentration of organic anions also has an impact on the organicization of Mnt. At a 1:1 ratio of SDS to CTAB, and at an SDS dosage <2 CEC, intercalation increased slightly as the SDS concentration increased (Fig. 5). However, as the concentration of SDS increased to >2 CEC, intercalation obviously increased and d_{001} in organic Mnt was as high as 34 Å. CTAB enters the Mnt interlayer through ion exchange and forms an organic environment, supplying a driving force for intercalation with Mnt. SDS is negatively charged, thus it partially forms a mixed micelle via interactions with CTAB and becomes partially adsorbed on the surface of Mnt. Both processes enhance the stability of the Mnt structure and promote organicization (İşçi et al. 2008).

The viscosity of organic Mnt also increased as the concentration of organics increased, reaching a maximum value of 395 mP·s with SDS of 2.5 CEC; the viscosity decreased as the concentration increased further. The above results suggest that the viscosity of organic Mnt is positively correlated with intercalation but is still related to organicization of the outer Mnt surface.

Influence of chain-length in organic anions The chain-length of organic cations or anions is also a key factor in the modification of Mnt (Fig. 6). The organic anions used in this study contain 12 or 16 carbon atoms, while other organic cations may also contain 8, 14, or 18 carbon atoms. The Mnt interlayer spacing changes with modification (Fig. 6). Longer chain-lengths of organic cations lead to a larger increase in the interlayer spacing.

In contrast, the chain-lengths of the organic anions have a negligible influence on the viscosity in modified Mnt. Mnt modified with organic anions containing 16 carbons has higher viscosity than that modified with 12 carbons. Organic Mnt exhibits the highest viscosity (395 mP·s) when modified using organic cations and anions with 12 carbon atoms. Increasing the chain-length further does not lead to greater viscosity. The result also indicates that the viscosity of organic Mnt is correlated with intercalation but is not completely determined by intercalation (Dultz et al. 2005).

Molecular Dynamic Simulation of Organic Mnt

Influence of Organic Cation Concentration The XRD pattern indicates that organics intercalate in the interlayer of Mnt. Further investigations, such as studies of the interaction between organics and Mnt, arrangement of interlayer organics, and combination of organics with the outer surface, require molecular dynamics simulations. Intercalation occurred between Mnt and organics at concentrations of 4, 1, and 0.2 CEC. Na^+ from the original Mnt diffuses into the aqueous solution, making Mnt electrically unbalanced with negative charge. Therefore, organic cations enter the Mnt interlayer through electronic attraction and gradually increase the interlayer spacing (Fig. 7).

During the process of intercalation of organic cations into Mnt, interlayer cations diffuse into aqueous solution, and water molecules enter the interlayer spacing, causing it to increase (Zeng et al. 2003; Zhou et al. 2012). This is also a factor in promoting the intercalation of organic cations. Some of the organic cations enter the interlayer, while some are adsorbed on the Mnt surface (Irannajad & Haghighi 2017). The amount of CTAB adsorbed on the surface and in the interlayer is influenced by its concentration. In the simulation, eight CTAB molecules enter the interlayer, three adsorb on the edge, and five are free in the solution at a concentration of 4 CEC.

At a concentration of 2.5 CEC, six CTAB enter the interlayer, while four adsorb on the edge. In contrast, more CTAB adsorbs on the Mnt edge at a concentration of 2.5 CEC than at 4 CEC. This produces stronger organicization and increases the interlayer spacing and viscosity. However, at a concentration of 0.2 CEC, all the CTAB enters the Mnt interlayer without adsorption on the edge. Thus, the result was caused by relatively weak organicization, lower interlayer spacing, and viscosity.

Influence of organic anion concentration The viscosity of the modified Mnt is largest when the effects of organic cations and anions are combined. Mixed solutions of organic cations and anions (with a ratio of 5:5) at 4 CEC (16), 2.5 CEC (10), and 1 CEC (4) to modify Mnt (Figure 8) were simulated. Organic cations enter the Mnt interlayer via ion exchange, while organic anions enter the interlayer through interactions between organic molecules. Ten organic cations and six anions enter the interlayer, two cations and two anions are adsorbed on the Mnt edge, and the remaining organic ions are dispersed in solution at a concentration of 4 CEC. Ions adsorbed on the outer surface interact with each other and enhance organicization of Mnt.

At a concentration of 2.5 CEC, six CTAB interlayer, and four cations and five anions adsorb on the edge. All organics interact with Mnt, yielding better organicization than at 4 CEC and resulting in organic Mnt with the highest viscosity. No interactions arise between organics at a concentration of 0.2 CEC because all organic ions enter the Mnt interlayer. These results suggest that an overdose of organic ions impedes organicization, and the viscosity of modified Mnt is maximized at a specific concentration and specific cation to anion ratio (Gűngőr et al. 2001; Tunç & Duman 2008).

CONCLUSIONS

Organic cations and anions were used to modify Mnt and prepare organic Mnt with high viscosity. The type and ratio of organics are key factors that influence the structure and performance of modified Mnt. The highest viscosity of organic Mnt (395 mP.s) was found at a 2.5 CEC concentration of cations and anions, pH 12, and organic chain length of 12 carbons. The XRD results and molecular dynamics simulations showed that ions intercalated the interlayer or were adsorbed on the outer surface. The viscosity of organic Mnt was influenced by the type of organics and by the amount of organics adsorbed on the outer surface. The latter had a greater effect than the former. Preparing and investigating high-viscosity, modified Mnt may encourage the use of organic Mnt in paint, drilling mud, or other applications.

ACKNOWLEDGEMENTS

This research was jointly funded by China Postdoctoral Science Foundation funded project (2018M631818) and the Doctoral Startup Foundation of Liaoning (20170520315).

REFERENCES

Alemdar, A., Őztekin, N., & Gűngőr, N. (2005). Effects of polyethyleneimine adsorption on the rheological properties of purified bentonite suspensions. *Colloids and Surfaces A: Physicochemical and Engineering Aspects, 252*, 95–98.

Austin, J. C., Perry, A., Richter, D. D., & Schroeder, P. A. (2018). Modifications of 2:1 clay minerals in kaolinite-dominated ultisol under changing land-use regimes. *Clays and Clay Minerals, 66*, 61–73.

Bumbudsanpharoke, N., Lee, W., Choi, J. C., & Park, S. J. (2017). Influence of montmorillonite nanoclay content on the optical, thermal, mechanical, and barrier properties of low-density polyethylene. *Clays and Clay Minerals, 65*, 387–397.

Dultz, S., Riebe, B., & Bunnenberg, C. (2005). Temperature effects on iodine adsorption on organo-clay minerals: II. Structural effects. *Applied Clay Science, 28*, 17–30.

Gűngőr, N., Alemdar, N., & Atici, O. (2001). The effect of SDS surfactant on the flow and zeta potential of bentonite suspensions. *Materials Letters, 51*, 250–254.

Günister, E., İşçi, S., Őztekin, N., Erim, F. B., Ece, Ő. I., & Gűngőr, N. (2006). Effect of cationic surfactant adsorption on the rheological and surface properties of bentonite dispersions. *Journal of Colloid and Interface Science, 303*, 137–141.

He, H., Frost, R. L., Bostrom, T., Yuan, P., Duong, L., & Yang, D. (2006) Changes in the morphology of organoclays with $HDTMA^+$ surfactant loading. *Applied Clay Science, 31*, 262–271.

Irannajad, M. & Haghighi, H. K. (2017). Removal of Co^{2+}, Ni^{2+}, and Pb^{2+} by manganese oxide-coated zeolite: equilibrium, thermodynamics, and kinetics studies. *Clays and Clay Minerals, 65*, 52–62.

İşçi, S., Gűner, F. S., & Güngör, N. (2005). Investigation of rheological and collodial properties of bentonitic clay dispersion in the presence of a cationic surfactant. *Progress in Organic Coatings, 54*, 28–33.

İşçi, S., Günister, E., Alemdar, A., Ece, Ö. I., & Güngör, N. (2008). The influence of DTABr surfactant on the electrokinetic and rheological properties of soda-activated bentonite dispersions. *Materials Letters, 62*, 81–84.

Jeschke, F. & Meleshyn, A. (2011). A Monte Carlo study of interlayer and surface structures of tetraphenylphosphonium-modified Na-montmorillonite. *Geoderma, 169*, 33–40.

Kaci, A. & Chaouche, M. (2011). Influence of bentonite clay on the rheological behaviour of fresh mortars. *Cement and Concrete Research, 41*, 373–379.

Karataş, D., Tekin, A., & Çelik, M. S. (2017). Density functional theory computation of organic compound penetration into sepiolite tunnels. *Clays and Clay Minerals, 65*, 1–13.

Kwolek, T., Hodorowicz, M., Stadnicka, K., & Czapkiewicz, J. (2003). Adsorption isotherms of homologous alkyldimethylbenzylammonium bromides on sodium montmorillonite. *Journal of Colloid and Interface Science, 264*(1), 14–19.

Lagaly, G. (1982). Layer charge heterogeneity in vermiculites. *Clays and Clay Mineral, 30*, 215–222.

Lv, G. C., Liu, L., Li, Z. H., Liao, L. B., & Liu, M. T. (2012). Probing the interactions between chlorpheniramine and 2:1 phyllosilicates. *Journal of Colloid and Interface Science, 374*, 218–225.

Martín Alfonso, J. E., Valencia, C., & Franco, J. M. (2014). Composition-property relationship of gel-like dispersions based on organo-bentonite, recycled polypropylene and mineral oil for lubricant purposes. *Applied Clay Science, 87*(1), 265–271.

Menezes, R. R., Marques, L. N., Campos, L. A., Ferreira, H. S., & Santana, L. N. (2010). Use of statistical design to study the influence of CMC on the rheological properties of bentonite dispersions for water-based drilling fluids. *Applied Clay Science, 49*, 13–20.

Ouhadi, V. R., Yong, R. N., & Sedighi, M. (2006). Influence of heavy metal contaminants at variable pH regimes on rheological behaviour of bentonite. *Applied Clay Science, 32*, 217–231.

Pospíšil, M., Čapková, P., Weissmannová, H., Klika, Z., & Trchová, M. (2003). Structure analysis of montmorillonite intercalated with rhodamine B: modeling and experiment. *Journal of Molecular Modeling, 9*(1), 39–46.

Tunç, S. & Duman, O. (2008). The effect of different molecular weight of poly (ethylene glycol) on the electrokinetic and rheological properties of Na-bentonite suspensions. *Colloids and Surfaces A: Physicochemical and Engineering Aspects, 317*, 93–99.

Vassilios, C., Kelessidis, C., Cassiani, P., & Antonios, F. (2009). Application of Greek lignite as an additive for controlling rheological and filtration properties of water–bentonite suspensions at high temperatures: A review. *International Journal of Coal Geology, 77*, 394–400.

Wu, L. M., Tong, D. S., & Zhao, L. Z. (2014a). Fourier transform infrared spectroscopy analysis for hydrothermal transformation of microcrystalline cellulose on montmorillonite. *Applied Clay Science, 95*(3), 74–82.

Wu, L. M., Liao, L. M., Lv, G. C., Qin, F. X., & Li, Z. H. (2014b). Microstructure and process of intercalation of imidazolium ionic liquids into montmorillonite. *Chemical Engineering Journal, 236*, 306–313.

Wu, L. M., Zhou, C. H., Tong, D. S., Yu, W. H., & Wang, H. (2014c). Novel hydrothermal carbonization of cellulose catalyzed by montmorillonite to produce kerogen-like hydrochar. *Cellulose, 21*(4), 2845–2857.

Wu, L. M., Yang, C. X., Mei, L. F., Qin, F. X., Liao, L. B., & Lv, G. C. (2014d). Microstructure of different chain length ionic liquids intercalated into montmorillonite: a molecular dynamics study. *Applied Clay Science, 99*, 266–274.

Wungu, T. D. K., Aspera, S. M., David, M. Y., Dipojono, H. K., Nakanishi, H., & Kasai, H. (2011). Absorption of lithium in montmorillonite: a density functional theory (DFT) study. *Journal of Nanoscience and Nanotechnology, 11*(4), 2793–2801.

Yalçin, T., Alemdar, A., Ece, Ö. I., & Güngör, N. (2002). By particle interactions and rheological properties of bentonites+ALS suspensions. *Materials Letters, 53*, 211–215.

Yoshimoto, S., Ohashi, F., & Kameyama, T. (2005). X-ray diffraction studies of intercalation compounds prepared from aniline salts and montmorillonite by a mechanochemical processing. *Solid State Communications, 136*, 251–256.

Yu, W. H., Ren, Q. Q., Tong, D. S., Zhou, C. H., & Wang, H. (2014). Clean production of CTAB-montmorillonite: formation mechanism and swelling behavior in xylene. *Applied Clay Science, 97-98*, 222–234.

Yu, W. H., Zhu, T. T., Tong, D. S., Wang, M., Wu, Q. Q., & Zhou, C. H. (2017). Preparation of organo-montmorillonites and the relationship between microstructure and swellability. *Clays and Clay Minerals, 65*, 417–430.

Zeng, Q. H., Yu, A. B., Lu, G. Q., & Standish, R. K. (2003). Molecular dynamics simulation of organic−inorganic nanocomposites: layering behavior and interlayer structure of organoclays. *Chemistry of Materials, 15*(25), 4732–4738.

Zhou, C. H. (2011). Cheminform abstract: Strategies towards clay-based designer catalysts for green and sustainable catalysis. *Cheminform, 42*(47), https://doi.org/10.1002/chin.201147260.

Zhou, C. H. & Keeling, J. (2013). Fundamental and applied research on clay minerals: From climate and environment to nanotechnology. *Applied Clay Science, 74*, 3–9.

Zhou, C. H., Shen, Z. F., Liu, L., & Liu, S. (2011). Preparation and functionality of clay-containing films. *Journal of Materials Chemistry, 21*(39), 15132–15153.

Zhou, C. H., Zhao, L. Z., Wang, A. Q., Chen, T. H., & He, H. P. (2016). Current fundamental and applied research into clay minerals in China. *Applied Clay Science, 119*, 3–7.

Zhou, C. H., Zhou, Q., Wu, Q. Q., Petit, S., Jiang, X. C., Xia, S. T., Li, C. S., & Yu, W. H. (2019). Modification, hybridization and applications of saponite: An overview. *Applied Clay Science, 168*, 136–154.

Zhou, J. H., Lu, X. C., Zhu, X. Z., Liu, X. D., Wei, J. M., & Zhou, Q. (2012). Interlayer structure and dynamics of HDTMA(+)-intercalated rectorite with and without water: a molecular dynamics study. *The Journal of Physical Chemistry C, 116*(24), 13071–13078.

Zhou, L. M., Chen, H., Jiang, X. H., Lu, F., Zhou, Y., & Yin, W. (2009). Modification of montmorillonite surfaces using a novel class of cationic Gemini surfactants. *Journal of Colloid and Interface Science, 332*(1), 16–21.

Zhou, Q., Shen, W., Zhu, J.X., Zhu, R.L., He, H.P., Zhou, J.H., & Yuan, P. (2014). Structure and dynamic properties of water saturated CTMA-montmorillonite: molecular dynamics simulations. *Applied Clay Science, 97*, 62–71.

Zhu, T. T., Zhou, C. H., Kabwe, F. B., Wu, Q. Q., Li, C. S., & Zhang, J. R. (2019). Exfoliation of montmorillonite and related properties of clay/polymer nanocomposites. *Applied Clay Science, 169*, 48–66.

[*Received 30 January 2019; revised 8 June 2019; AE: Chun-Hui Zhou*]